S55E-0196

Better earthquake forecasting in Southern California by joint resolving of the fault plane ambiguity and anisotropic earthquake triggering?

Leila Mizrahi[1]; Shyam Nandan[1]; Stefan Wiemer[1]

[1]Swiss Seismological Service, ETH Zurich; leila.mizrahi@sed.ethz.ch

1 *Starting point:*

Epidemic-Type Aftershock Sequence (ETAS) models…

…are the most successful earthquake forecasting models currently available, both for short- and long-term hazard assessment. They account for the spatio-temporal clustering of earthquakes intrinsically using basic **empirical triggering laws**.

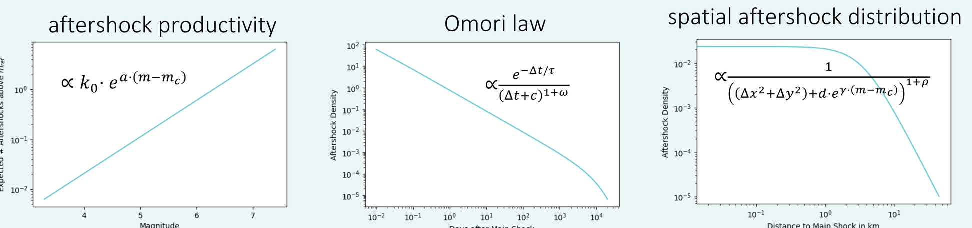

The rate λ of events at location (x, y) and time t is the sum of background event rate μ plus rate of aftershocks g of all previous events.

$$\lambda(x, y, t) = \mu + \sum_{i: t_i < t} g(m_i, t - t_i, x - x_i, y - y_i),$$

$$g(m, \Delta t, \Delta x, \Delta y) = \frac{k_0 \cdot e^{a \cdot (m - m_c)}}{\left((\Delta x^2 + \Delta y^2) + d \cdot e^{\gamma \cdot (m - m_c)}\right)^{1+\rho}} \cdot \frac{e^{-\frac{\Delta t}{\tau}}}{(\Delta t + c)^{1+\omega}}.$$

2 *Ultimate goal:*

Better earthquake forecasting

How do we get there?

…by developing **ideas** for better forecasting models, **implementing** those ideas, and **testing** the forecasting power of new models versus current state-of-the-art.

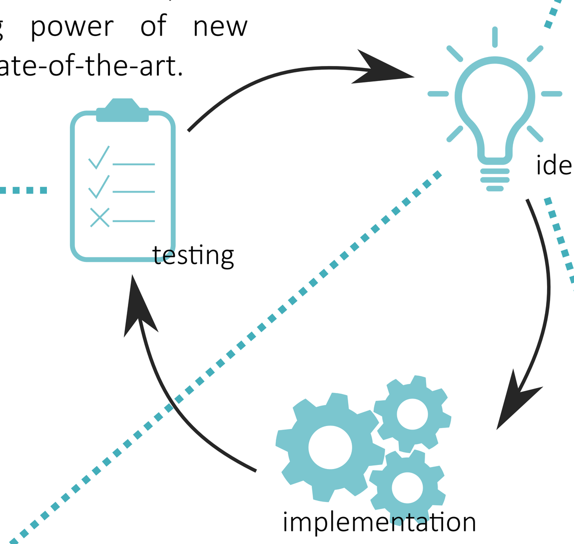

3 *ETAS + X*

as a multifunctional tool

Developing self-consistent ETAS + X models allow us to…

- (hopefully) **improve forecasting**
- **invert for** X in a way that is consistent with earthquakes' triggering behavior
- better **understand** X, and better **understand seismicity**, based on where and when ETAS + X does or does not outperform the null model

4 *How do we test new models?*

Using pseudo-prospective forecasting experiments.

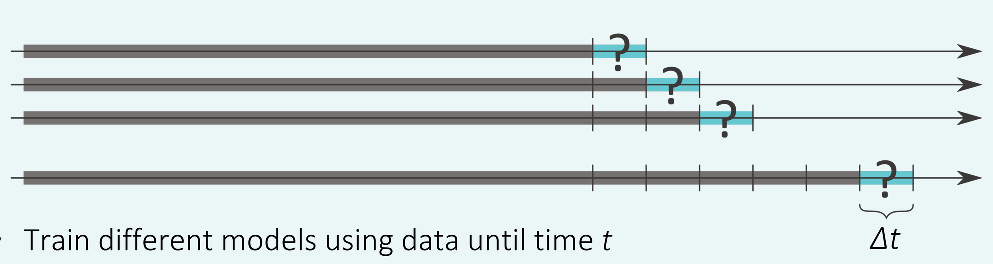

- Train different models using data until time *t*
- Issue forecasts for testing period *[t, t+Δt]*
- Compare forecasts to actual data during testing period
- Repeat for multiple testing periods

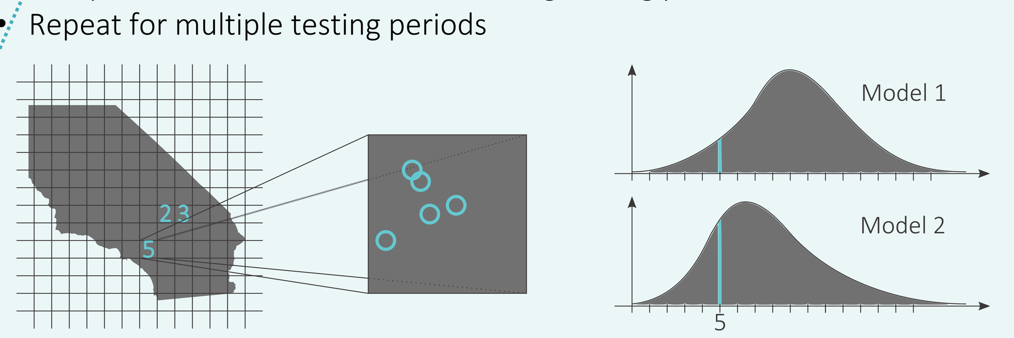

Forecast evaluation (see *Nandan et al., 2019a*):

- In each grid cell, count the number of events that actually happened
- Calculate the likelihood of this to occur under each of the models (M1, M2), based on 100,000 simulations
- Information gain of M1 vs M2: difference in log likelihood, summed over all grid cells

7 *Up next: ETAS - X*

Instead of further constraining the model, we plan to give it more freedom and allow productivity and background rate to vary with space, with time, with sequences, in fact, with each event.

…and how would you develop next-generation earthquake forecasting models?

5A *ETAS + focal mechanisms (FM)*

We tackle two problems at once:

- Knowing the focal mechanism of an event, we introduce ETAS with anisotropic aftershock triggering.
- Knowing the triggering relationships between all events of a catalog (as a result of ETAS parameter calibration), we infer the plausibility of each of the two specified fault planes.

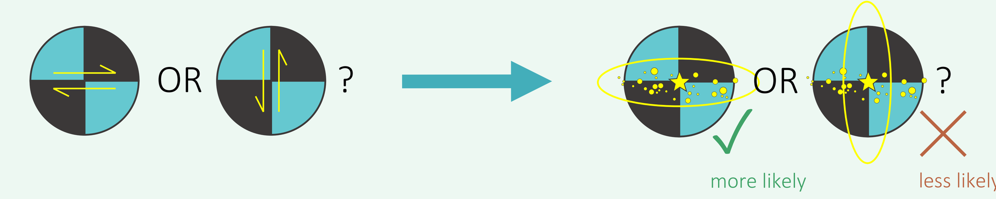

We developed an enhanced ETAS model with two modifications:

- **elliptical aftershock triggering** kernel. Locations with equal aftershock rates g lie on an ellipse around their parent event.

$$g \propto \frac{1}{\left((\Delta x^2 + \Delta y^2) + d \cdot e^{\gamma \cdot (m - m_c)}\right)^{1+\rho}} \qquad g \propto \frac{1}{\left(\left(\frac{\Delta x^2}{e^{\varepsilon(m - m_c) + \delta}} + \Delta y^2\right) + d \cdot e^{\gamma \cdot (m - m_c)}\right)^{1+\rho}}$$

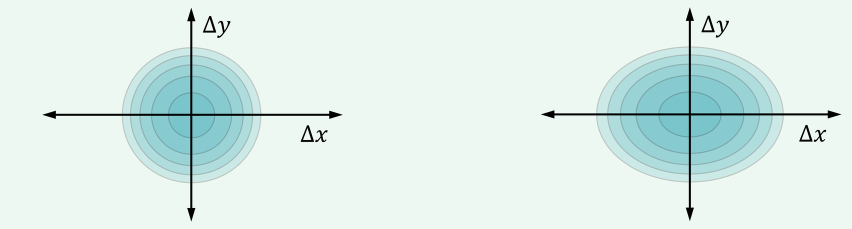

Figure 1: Locations with equal aftershock rate when assuming isotropic triggering (left) and elliptic triggering (right). Δx: distance to parent event in direction of parent strike, Δy: distance in direction perpendicular to strike.

- During ETAS parameter calibration, we treat each source event with available FM as two separate events, corresponding to the two possible fault planes induced by the FM solution. The **plausibility of each plane** is then proportional to the number of aftershocks it can explain.

5B

Experiment setup

- 2 competing models (elliptic/isotropic ETAS)
- Southern California, 1981 – 2020 (catalog: Yang et al., 2012 with FM)
- 243 non-overlapping 30 day forecast testing periods, January 1[st], 2000, ending January 2020
- Spatial resolution: 0.1° lat x 0.1° long (≈ 10km x 10km)

5C

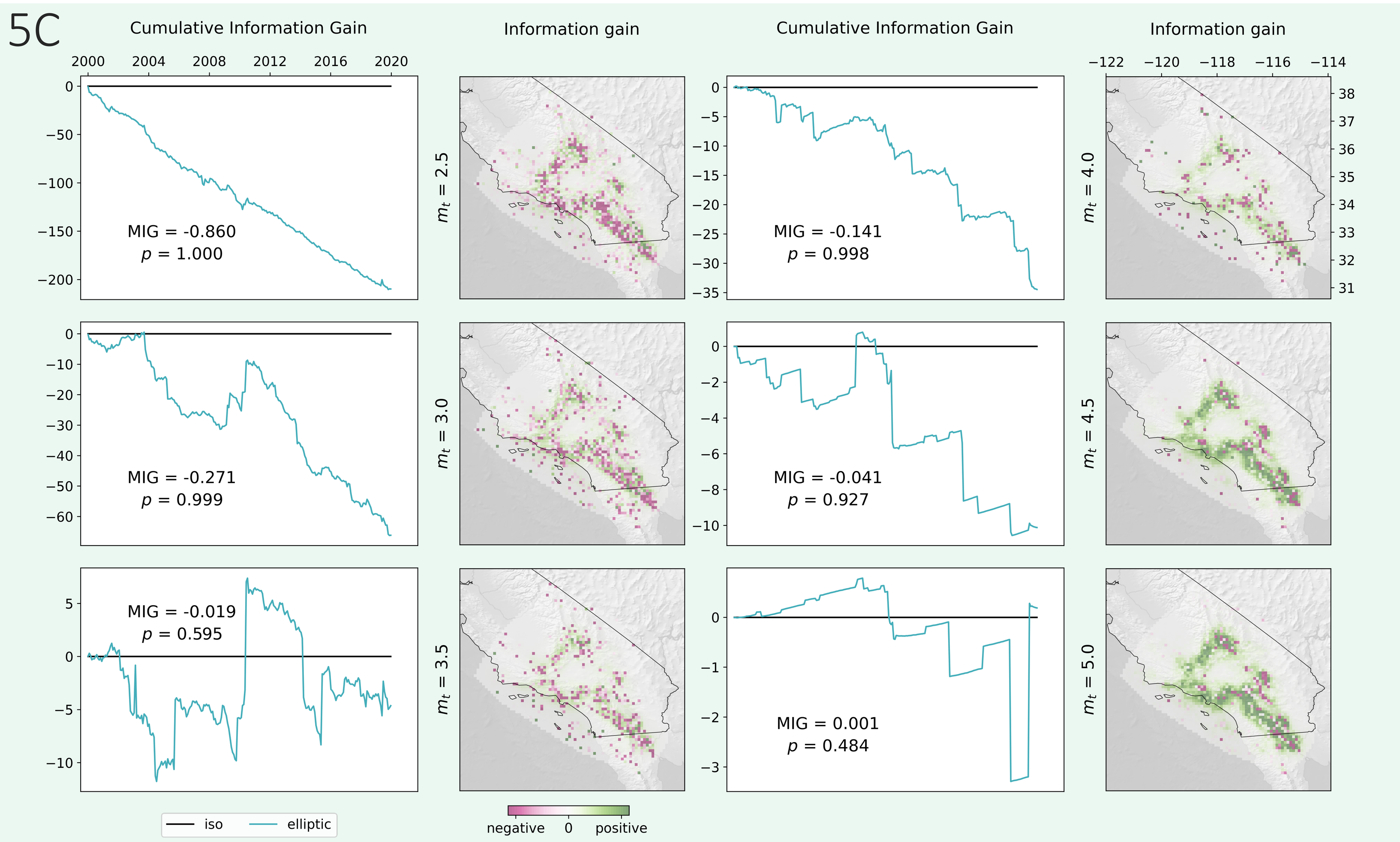

Figure 2 (above): Cumulative information gain (over time) and total information gain (in space) of the anisotropic ETAS versus isotropic ETAS model, for different target magnitude thresholds m_t. Mean information gain (MIG) and p-value testing the superiority of the anisotropic model are given.

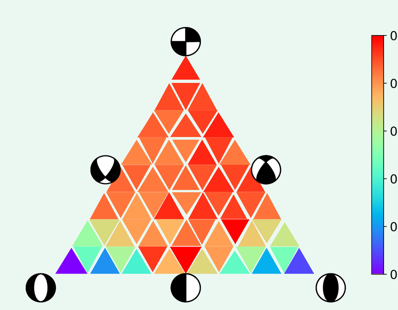

Figure 3 (left): Mean weight of the dominant nodal plane for different groups of focal mechanisms.

Figure 4 (right): Focal mechanisms of the four largest events in the catalog and their aftershocks (dots). Dot size reflects likelihood to be triggered by the mainshock, dot color reflects likelihood to be triggered by each of the nodal planes. Overall weight of each nodal plane is indicated in the color bar legend.

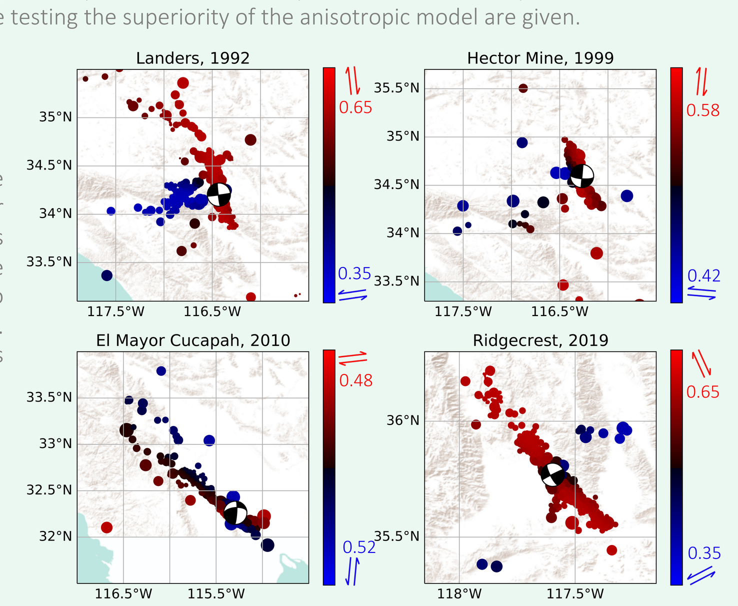

Results & conclusions

- Elliptic ETAS with FMs **does not outperform** isotropic ETAS
- Next steps: accounting for different **faulting styles,** increase relevance of dominant nodal plane when simulating, etc.

6A *ETAS + short-term aftershock incompleteness (STAI)*

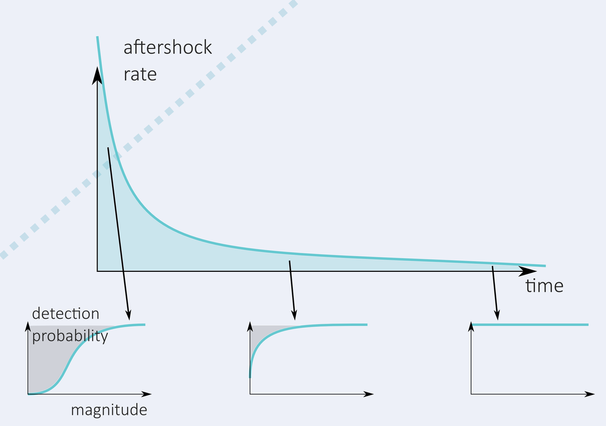

Figure 5: Detection probability is lower for small magnitude events, and during times when event rate is high.

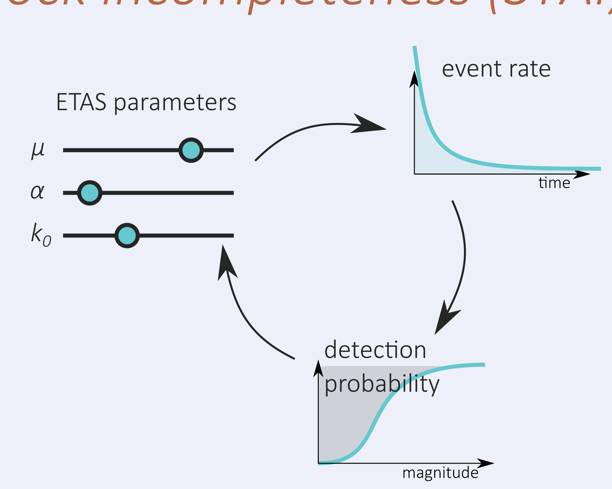

Figure 6: Simplified schematic illustration of the inversion algorithm.

Algorithm 1: Jointly estimate high-frequency detection incompleteness and ETAS parameters:

1. Estimate ETAS assuming constant M_c
2. Calculate rates, accounting for fraction of unobserved events ($\xi(t_i)$):

$$\Lambda(t) = \iint_R \mu \, dx \, dy + \sum_{i: t_i < t} (1 + \xi(t_i)) \cdot \iint_R g(m_i, t - t_i, x - x_i, y - y_i) \, dx \, dy$$

3. Calibrate detection probability, update $\xi(t_i)$
4. Re-estimate ETAS parameters knowing high-frequency detection probability
5. Repeat from 2. until convergence

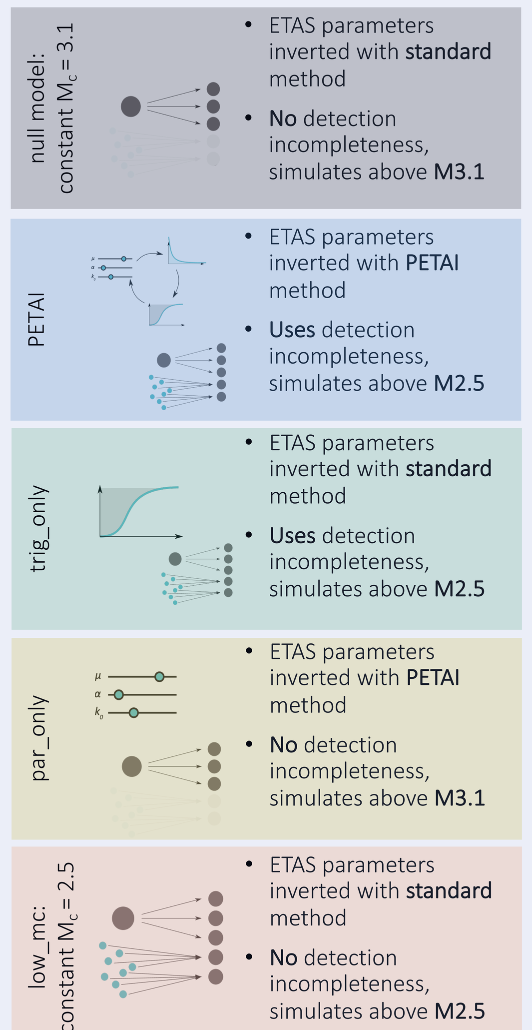

6B

Experiment setup

Same as **5B** (above) but:

←5 competing models

- California, 1970 – 2020 (catalog: ComCat)

more soon in: Mizrahi et al., 2021 (accepted)

6C

Results & conclusions

Figure 7 (right): Cumulative information gain (IG) of the 4 alternative models vs. null ETAS model for different target magnitudes. Below each plot, mean IG and t-test p-value (testing whether base model is outperformed) are given for the 4 alternative models. The competing models are described below.

m_t = 3.1

	mean IG	p-value
PETAI	0.97	0.00
trig_only	0.94	0.00
par_only	-0.12	0.94
low_mc	0.27	0.42

m_t = 3.5

	mean IG	p-value
PETAI	0.05	0.35
trig_only	0.12	0.18
par_only	-0.14	1.00
low_mc	-0.30	0.62

m_t = 4.0

	mean IG	p-value
PETAI	-0.03	0.65
trig_only	0.02	0.37
par_only	-0.05	0.97
low_mc	-0.04	0.53

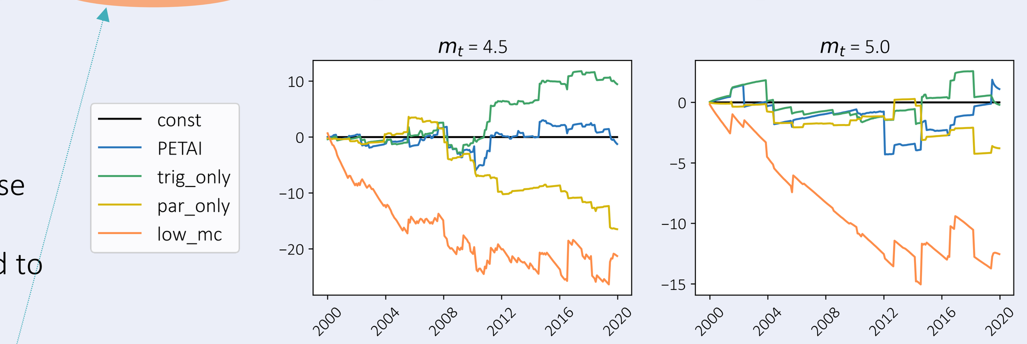

m_t = 4.5

	mean IG	p-value
PETAI	-0.01	0.56
trig_only	0.04	0.11
par_only	-0.07	0.98
low_mc	-0.09	0.61

m_t = 5.0

	mean IG	p-value
PETAI	0.00	0.42
trig_only	-0.00	0.52
par_only	-0.02	0.81
low_mc	-0.05	0.66

- For m_t = 3.1, **allowing small event triggering significantly improves the forecast.**
- For larger thresholds, this is not the case anymore.

→ Possible explanation: earthquakes tend to preferentially trigger similarly sized aftershocks (see *Nandan et al., 2019b*).

- **Accounting for incompleteness is necessary** to achieve the improvement (simply assuming lower M_c doesn't do the job).

References

Mizrahi L., Nandan, S., Wiemer, S. 2021. Embracing Data Incompleteness for Better Earthquake Forecasting. *Journal of Geophysical Research: Solid Earth.* (accepted)

Nandan, S., Ouillon, G., Sornette, D. and Wiemer, S., 2019a. Forecasting the full distribution of earthquake numbers is fair, robust, and better. *Seismological Research Letters*, 90(4), pp.1650-1659.

Nandan, S., Ouillon, G. and Sornette, D., 2019b. Magnitude of earthquakes controls the size distribution of their triggered events. *Journal of Geophysical Research: Solid Earth*, 124(3), pp.2762-2780.

Yang, W., Hauksson, E., & Shearer, P. M. (2012). Computing a large refined catalog of focal mechanisms for southern California (1981–2010): Temporal stability of the style of faulting. *Bulletin of the Seismological Society of America*, 102(3), 1179-1194.

Acknowledgements

This work has received funding from the Eidgenössische Technische Hochschule (ETH) research grant for project number 2018-FE-213, "Enabling dynamic earthquake risk assessment (DynaRisk)" and from the European Union's Horizon 2020 research and innovation program under Grant Agreement Number 821115, real-time earthquake risk reduction for a resilient Europe (RISE).

Schweizerischer Erdbebendienst
Service Sismologique Suisse
Servizio Sismico Svizzero
Swiss Seismological Service

ETH zürich

RISE — Real-time earthquake risk reduction for a resilient Europe